Int J Clin Exp Pathol 2019;12(2):431-442
www.ijcep.com /ISSN:1936-2625/IJCEP0087815

Original Article

The overexpression of MYST4 in human solid tumors is associated with increased aggressiveness and decreased overall survival

Chao-Lien Liu[1*], Jim Jinn-Chyuan Sheu[2,3,5*], Hsuan-Ping Lin[7], Yung-Ming Jeng[6,7], Cherry Yin-Yi Chang[4], Chih-Mei Chen[3], Jack Cheng[3], Tsui-Lien Mao[6,7]

[1]School of Medical Laboratory Science and Biotechnology, College of Medical Science and Technology, Taipei Medical University, Taipei, Taiwan; [2]Institute of Biomedical Sciences, National Sun Yat-sen University, Kaohsiung, Taiwan; [3]Human Genetic Center, [4]Department of Obstetrics and Gynecology, China Medical University Hospital, Taichung, Taiwan; [5]Department of Health and Nutrition Biotechnology, Asia University, Taichung, Taiwan; [6]Department of Pathology, National Taiwan University Hospital, Taipei, Taiwan; [7]Department of Pathology, College of Medicine, National Taiwan University, Taipei, Taiwan. [*]Equal contributors.

Received November 3, 2018; Accepted November 26, 2018; Epub February 1, 2019; Published February 15, 2019

Abstract: MYST4 (also called MORF and KAT6B) is one of the histone acetyltransferases with transcriptional regulatory activity. It was found to be overexpressed in ovarian cancer by a serial analysis of gene expression assays that focused on plant homeodomain-linked domain-containing genes. Compared to ovarian clear cell carcinomas and endometrioid carcinomas, MYST4 is significantly overexpressed in ovarian high-grade serous carcinomas (HGSCs) and was correlated with diminished patient survival in advanced stage HGSCs. Due to limited data on MYST4 in tumorigenesis and tumor progression, we explored the functional roles of MYST4 in human tumors. Besides the ovarian cancer cell line A2780, we chose two other types of human cancer cell lines expressing high mRNA levels of MYST4, SKBR3 and Huh7, for further *in vitro* investigation. Athymic *nu/nu* mice were utilized to facilitate the *in vivo* xenograft study. To search for potentially regulated genes, a microarray study comparing the expression profile before and after MYST4 knockdown was performed. Overexpression of MYST4 in HCCs was significantly associated with decreased survival. The knockdown of MYST4 significantly reduced cellular proliferation, migration, and cell cycle progression in all three cancer cell lines. Moreover, the knockdown of MYST4 in Huh7 cells suppressed tumor growth in a mouse xenograft model. Furthermore, based on our microarray study, we identified several downstream genes important in regulating tumor behaviors. Collectively, our results suggest that MYST4 is involved in cancer progression and contributes to a more aggressive behavior in human solid tumors. Targeting MYST4 represents an appealing strategy for the effective treatment of advanced solid tumors overexpressing MYST4.

Keywords: MYST4, histone acetyltransferase, tumor progression

Introduction

Epigenetic alteration is one of the pathological processes that contribute to carcinogenesis, including DNA methylation, RNA-associated silencing, and histone modifications [1, 2]. Modifications of histones include acetylation, phosphorylation, methylation, ubiquitylation, and sumoylation [3]. Among these complex epigenetic regulatory mechanisms, histone acetyltransferases (HATs) [3, 4] play integral roles involving aberrant chromatin organization and therefore induce abnormal gene expression patterns resulting in cancer formation. HATs such as monocytic leukemic zinc-finger protein (MOZ) and MOZ-related factor (MORF; also known as MYST4) play important roles in chromatin package regulatory mechanisms including chromatin assembly, ATP-dependent remodeling, covalent modification, condensing-mediated condensation, and associations of noncoding RNAs [5-7]. From a cancer biology standpoint, it is important to understand the fundamental mechanisms whereby chromatin's structure and function are regulated.

Herein, we identified the overexpression of MYST4 in human ovarian carcinomas (OCs) by a

serial analysis of gene expression (SAGE) assay (Figure S1) focusing on plant homeodomain-linked (PHD) domain-containing genes. MYST4 (also known as MORF [8] and KAT6B [9]), the 4th member of the MOZ [10], Ybf2/Sas3 [11], Sas2, and TIP60 [12], (MYST) domain protein family, is the third major group of mammalian HATs which contain a putative acetyl-CoA-binding motif. There are five MYST proteins in humans, the structural features of which include an N-terminal part of the Enok, MOZ, or MORF (NEMM) domain, tandem PHD-linked zinc fingers, a long acidic stretch, and a serine/methionine-rich (SM) region. Functionally, the NEMM domain shows some sequence similarity to histones H1 and H5, but the function of this domain is not clear yet. In addition, studies showed that tandem PHD fingers can control the pluripotency of embryonic stem cells [13], possibly due to recognizing methyl-lysine-containing motifs [6]. Moreover, the SM domain possesses transcriptional activation; therefore, it was hypothesized that MYST4 is a transcriptional co-regulator [7, 8].

It is now known that the MYST4 protein plays important roles in various biological processes [14-16], including tumorigenesis. It is also well documented that the MYST4 gene is mutated in some developmental disorders, including Noonan syndrome-like disorder [17], Ohdo syndrome [18, 19], genitopatellar syndrome [20, 21] and blepharophimosis-ptosis-epicanthus inversus syndrome [22]. As to the most updated role of MYST4 in tumorigenesis, investigations showed that the MYST4 gene fused to the CBP gene via translocation t(10;16)(q22;p13) is associated with acute myeloid leukemia [23, 24]. In addition to circulating malignancies, MYST4 gene alteration was also found in solid tumors, such as leiomyomata [25, 26], breast cancer [27], and castration-resistant prostate cancer [28]. Therefore, genetic alternations of the MYST4 gene found in humans include translocation, mistargeted acetylation, and amplification. However, there is very scant evidence so far investigating the role of MYST4 in the development of solid tumors as well as any correlations with clinical significance.

In this present study, we found that MYST4 is overexpressed in ovarian HGSCs and HCCs, and its overexpression was significantly correlated with the decreased survival of clinical patients. Because MYST4 plays critical roles in cellular growth and developmental regulation, we investigated the role of MYST4 in three different types of human cancer cell lines overexpressing MYST4 and performed functional studies using a small hairpin RNA-knockdown approach. According to our results, MYST4-knockdown significantly reduced cellular proliferation and migration, and caused G_2/M cell cycle arrest in all three human cancer cell lines, including A2780 (OC), SKBR3 (breast carcinoma), and Huh7 (HCC) *in vitro*. For the *in vivo* study, the knockdown of MYST4 in Huh7 cells led to a significant inhibition of tumor growth in a mouse xenograft model. From our microarray study, we identified several significantly down-regulated genes in all three cell lines after the knockdown of MYST4. Collectively, our results suggest that MYST4 regulates solid tumor growth and progression, as well as diminishes patient survival, and therefore may serve as a potential treatment target in tumors overexpressing MYST4.

Materials and methods

Tissue materials

Fresh frozen tissues of OCs (45 HGSC, 17 endometrioid carcinoma (EM), and 27 clear cell carcinoma (CCC)) and 35 normal myometrial tissues were used for comparison of the mRNA levels of MYST4. Representative paraffin sections of 159 ovarian HGSCs and 89 HCCs were selected for immunohistochemical (IHC) analyses. The histological diagnosis was reviewed by TL Mao. The use of archival materials was approved by the ethics review board (approval number. 201112064RIC).

IHC

IHC was performed using a polyclonal antibody against MYST4 (Sigma-Aldrich, MO, USA at a 1:1000 dilution) on paraffin-embedded whole tissue sections. Antigen retrieval was performed by incubating slides in a citric acid buffer (pH 6.0) at 120°C for 10 min. The signal was visualized with the EnVision+ system (Dako, Carpentaria, CA, USA). The presence of nuclear staining was considered positive and further scored 0~3+ (0: negative; 1+: weak immunoreactivity; 2+: moderate immunoreactivity; 3+: strong immunoreactivity). Leydig cells from

human testicular tissue were used as a positive control.

Cell culture

All three cancer cell lines (ovarian carcinoma A2780, breast carcinoma SKBR3, and hepatocellular carcinoma Huh7) purchased from ATCC were maintained in Dulbecco's modified Eagle's medium (DMEM) supplemented with 10% heat-inactivated fetal bovine serum (FBS), 100 U/mL penicillin, 100 μg/mL streptomycin, non-essential amino acids, and 1 mM sodium pyruvate according to standard culture procedures. The cells were kept at 37°C in a humidified atmosphere composed of 95% air and 5% CO_2.

RNA isolation and quantitative real-time reverse transcription polymerase chain reaction (qRT-PCR)

Fresh frozen tissues or cell pellets were subjected to RNA extraction with an RNeasy mini kit (Qiagen, Valencia, CA, USA). RT was performed using a High Capacity cDNA Reverse Transcription kit (Applied Biosystems, Foster City, CA, USA). Quantitative real-time RT-PCR was then carried out with the ABI PRISM 7900HT Sequence Detection System (Applied Biosystems) using a QuantiTech SYBR green RT-PCR kit (Qiagen, Valencia, CA, USA). The primer sequences of MYST4 were: forward 5'-AACCTGTTCCAGAGCCAATG-3' and reverse 5'-TGTACTTTTGCAGGTGATTG-3'. Each sample was tested in triplicate, the expression level was normalized to an APP internal control (forward: 5'-GTGAAGATGGATGCAGAATTCCG-3' and reverse: 5'-AAAGAACTTGTAGGTTGGATTTTCG-3'), and the cycle difference was calculated by the delta-delta C(t) method.

RNA interference (RNAi)

To knock down endogenous MYST4, shRNA pLKO.1 vectors were transfected using a lentiviral system, with the envelope plasmid, pMD.G, and the packaging plasmid, pCMVDR8.91, into HEK 293T cells. Five shRNAs against MYST4 were first tested, and the following two had the highest knockdown effects and were selected for further study. The shRNA sequences of MYST4 were as follows: sh48 (TRCN0000245348) GATATTAGAAGTCGGTTTATT, and sh51 (TRCN0000245351) ATGGAAATGCCTCTAACTTTA. A shRNA vector against LacZ was used as a scrambled control. Transduced cells were selected with puromycin. RNAi reagents and shRNAs were obtained from the RNAi Core Facility of Academia Sinica (Taipei, Taiwan).

Flow cytometry for cell cycle analysis

Harvested cells were resuspended in phosphate-buffered saline (PBS) and then fixed in ice cold 70% alcohol. RNA was degraded with RNase, and the DNA content was stained with propidium iodide (Sigma-Aldrich). DNA ploidy was then analyzed by FACSCalibur flow cytometry (BD Biosciences, San Jose, CA, USA).

Migration assay

Cells were grown in six-well plates to confluence and scratched with a sterile pipette tip. After rinsing with a culture medium, the cells were re-incubated at 37°C. The migration distance was measured between the wounded edges every 12 h for 2 days.

Microarray study

Total RNA of 0.2 μg from each sample was amplified by a Low Input Quick-Amp Labeling kit (Agilent Technologies, USA) and labeled with Cy3 (CyDye, Agilent Technologies, USA) during the in vitro transcription process. Cy3-labled cRNA of 0.6 μg was fragmented to an average size of about 50-100 nucleotides by incubation with a fragmentation buffer at 60°C for 30 minutes. Correspondingly fragmented labeled cRNA was then pooled and hybridized to Agilent SurePrint G3 Human GE 8 × 60 K Microarray (Agilent Technologies, USA) at 65°C for 17 h. After washing and drying by nitrogen gun blowing, microarrays were scanned with an Agilent microarray scanner (Agilent Technologies, USA) at 535 nm for Cy3. The scanned images were analyzed by Feature extraction 10.5.1.1 software (Agilent Technologies, USA). Image analysis and normalization software was used to quantify the signal and background intensity for each sample.

In vivo studies

All mice were reared according to National Institutes of Health guidelines for animal care and guidelines of the Animal Center at China Medical University (ACCMU), and all animals were maintained in a specific pathogen-free

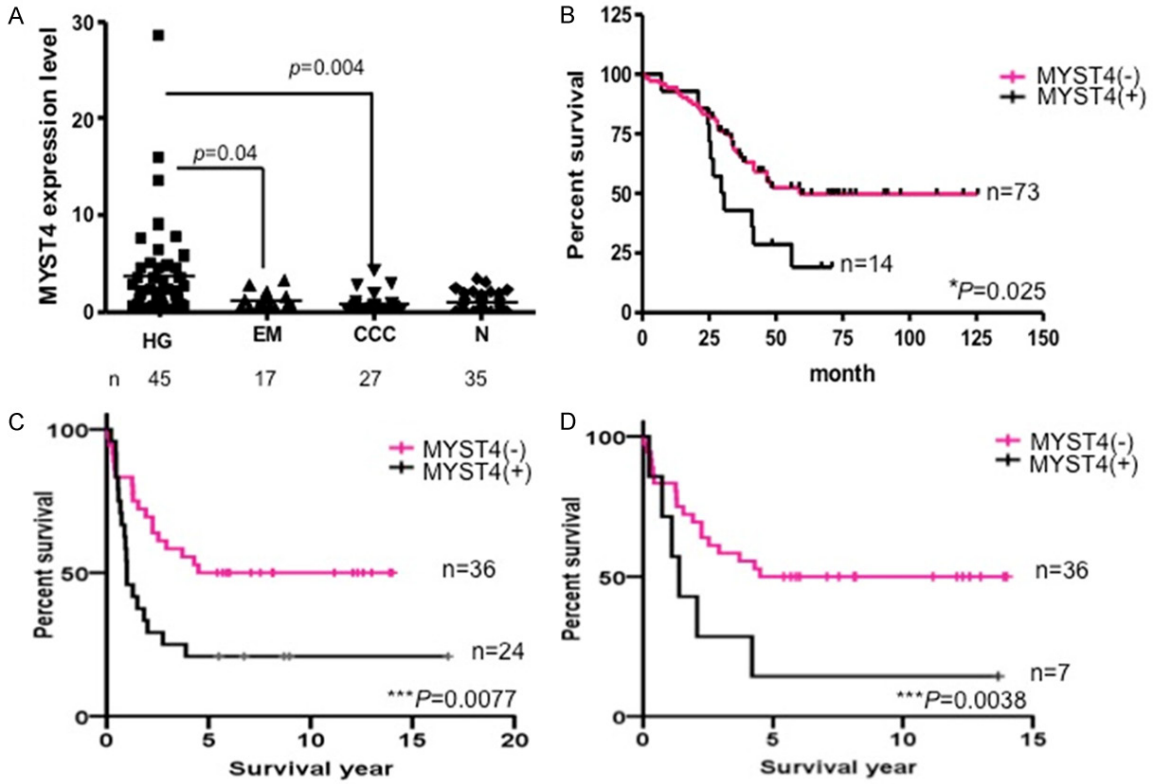

Figure 1. MYST4 is overexpressed in higher-grade cancers and was correlated with poor survival in both ovarian carcinoma (A, B) and hepatocellular carcinoma (HCC) patients (C, D). (A) MYST4 was significantly overexpressed in high-grade (HG) serous carcinomas (n=45) compared to endometrioid (EM) (n=17; P=0.04) and clear cell carcinomas (CCC) (n=27; P=0.04). N, normal tissue. (B) MYST4 expressed in advanced-stage ovarian HG serous carcinomas correlated with a reduction in overall survival (P=0.025). In HCC patients, (C) MYST4 1+ expression (n=24; ***P=0.0077) and (D) MYST4 3+ expression (n=7; ***P=0.0038) showed reduced overall survival compared to MYST4 non-expressing HCCs (n=36).

(SPF) facility. Six- to 8-week-old female athymic *nu/nu* mice were purchased from BioLASCO Taiwan Co., Ltd. and were randomized into different experimental groups. Huh7 cells transfected with either sh-MYST4-51 (clone 51) or the mock control (clone LacZ) were mixed with matrix gel (1:1 v/v) (Becton Dickinson) and then subcutaneously injected into the back of each mouse (10^7 cells per injection per mouse for the 6 mice per group). Tumor size was measured every 3 days, and tumor volume was estimated as width (mm) × length (mm) × height (mm). Nine weeks after cell inoculation, the mice were sacrificed, and their tumors were excised and weighed. All animal protocols were approved by the Institute Animal Care and Use Committee (IACUC) of CMU (approval number 101-24-N).

Statistical analysis

Survival analyses comparing the expression levels of MYST4 and patient survival were carried out with the Kaplan-Meier method and a log-rank test. The differences between two groups were evaluated using the paired Student's *t*-test. Categorical data were compared by Fisher's exact test. Three independent *in vitro* experiments were performed for each assay. Results are expressed as the mean ± standard deviation (SD). $P<0.05$ was considered statistically significant.

Results

MYST4 overexpression is correlated with HG carcinomas and reduced survival

In our pilot study, SAGE analysis of PHD domain-containing genes in OC cell lines and ovarian tumor tissues revealed several highly overexpressed genes, including HBXAP, PHF3, and MYST4 (Figure S1). MYST4, a HAT, was found to be overexpressed in OC14 OC tissue. To investigate the role of MYST4 in human carcinogenesis, we first compared the mRNA levels of

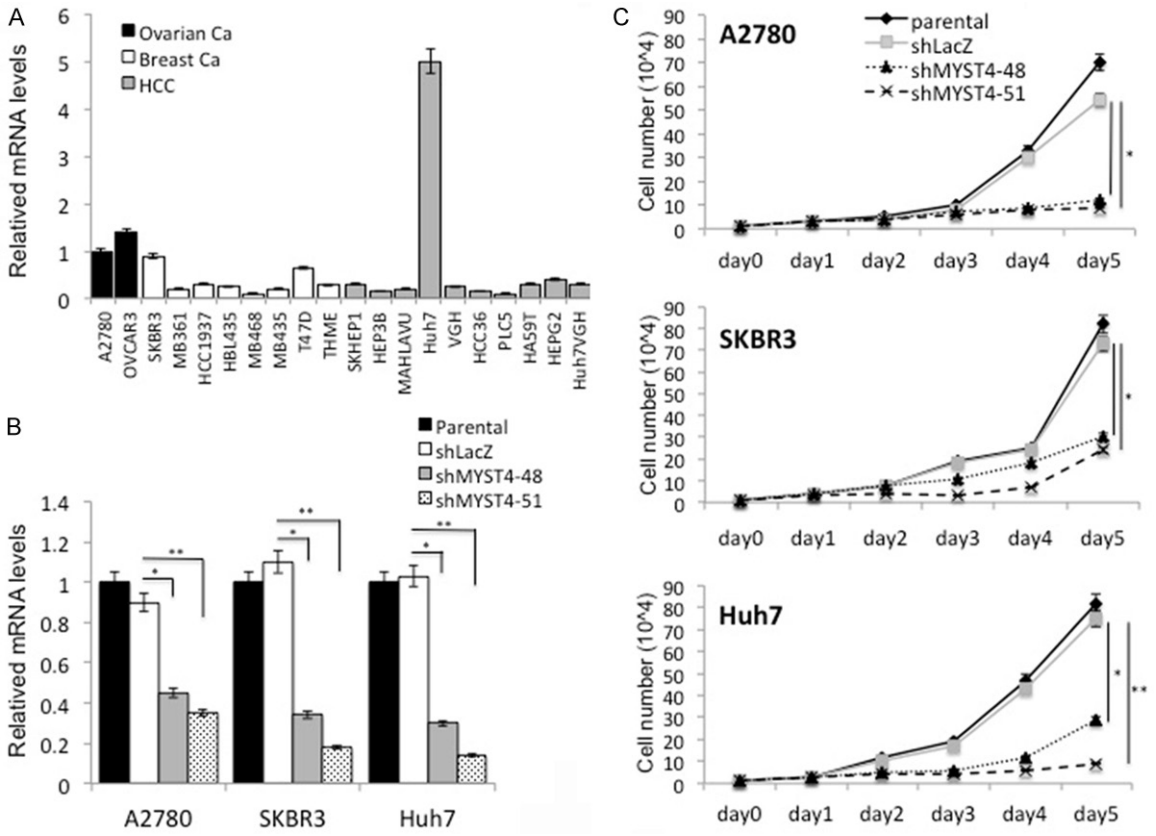

Figure 2. Comparisons of MYST4 expression levels, the knockdown efficiency, and suppressed cell proliferation following silencing in three selected-high MYST4-expressing cell lines. (A) Two ovarian cancer cell lines (A2780 and OVCAR3), eight breast cancer cell lines (SKBR3, MB361, HCC193, HBL435, MB468, MB435, T47D, and THME), and ten hepatocellular carcinoma (HCC) cell lines (SKHEP1, HEP3B, MAHLA, Huh7, VGH, HCC36, PLC5, HA59T, HEPG2, and Huh7VG) were used to identify MYST4 levels using an RT-qPCR. (B) Three different cancer cell lines (A2780, SKBR3, and Huh7) were selected for a further MYST4-knockdown investigation. shMYST4-48 and -51 clones showed significant MYST4 silencing efficacy compared to the control (sh*LacZ*) and parental cells. Data are presented as the mean ± SD of three independent experiments. **P*<0.05, ***P*<0.01. (C) Cells at 10^4 cells/well were seeded on day 0, and the number of cells was counted at different time points. Two MYST4-knockdown clones (shMYST4-48 and shMYST4-51) exhibited significantly reduced cell proliferation activities in human (C, upper panel) A2780 (ovarian cancer), (C, middle panel) SKBR3 (breast cancer), and (C, lower panel) Huh7 (liver cancer) cancer cell lines, compared to the mock control (sh*LacZ*) and parental cells. Data are presented as the mean ± SD of three to five independent experiments. **P*<0.05, ***P*<0.01.

MYST4 in several histological types of OCs by qRT-PCR. EM carcinomas and CCCs showed low levels of MYST4 expression, similar to those of normal myometrial tissues. In contrast, increased MYST4 expression was noted in some HGSCs. Overall, the levels of MYST4 were significantly higher in the HGSCs than they were in the EM carcinomas (*P*=0.04) and CCCs (*P*=0.004) (**Figure 1A**). The survival impact of the overexpression of MYST4 in OCs was further investigated by IHC in HGSCs. Expression of MYST4 was detected in 17% (27/159) of HGSCs. A survival analysis was performed for patients who presented with advanced-stage disease (FIGO stage III/IV). Only patients with at least 2 years of follow-up were included in the survival analysis to avoid comorbid factors. Patients with tumors expressing MYST4 had a significantly worse overall survival (*P*=0.025) (**Figure 1B**).

Since a high expression level of MYST4 was also found in the cancer cell line from HCC, we further investigated the correlation of the expression of MYST4 and survival in HCCs by IHC. In the 89 HCCs, 53 cases (59.6%) were positive for MYST4. Due to the high prevalence of MYST4 positivity, we further sub-classified these MYST4-expressing tumors into 3 scores, of which 24 showed 1+, 22 showed 2+, and

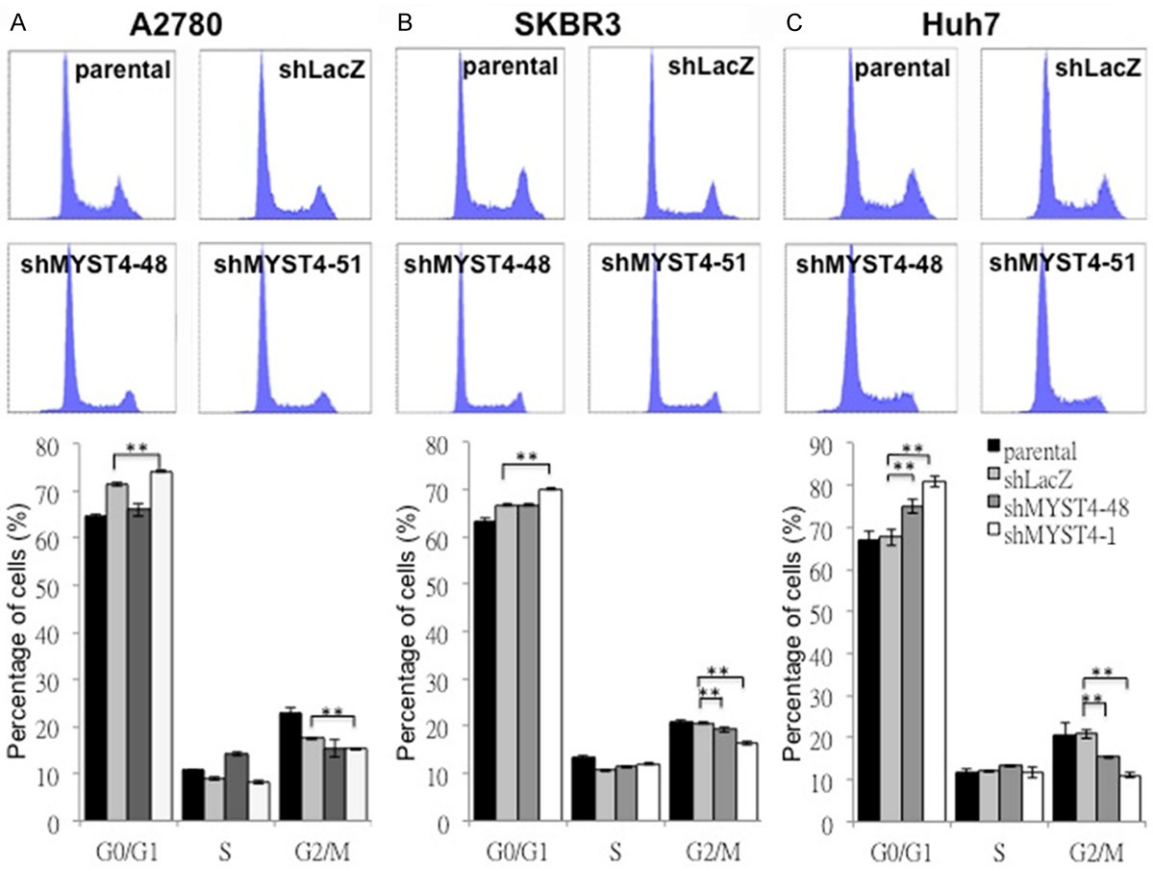

Figure 3. Investigation of the cell cycle distribution following MYST4 silencing in A2780, SKBR3, and Huh7 cells. (A-C upper panels) Propidium iodide staining shows that the silencing of MYST4 in cancer cells induced cell cycle arrest at the G_0/G_1 phase and blocked cell cycle progression according to a flow cytometric analysis. (A-C lower panels) Quantitative analysis of each cell cycle step after the flow cytometric analysis. Data are presented as the mean ± SD of three independent experiments. ***P*<0.01.

seven showed 3+ positivity. Of note, the positively stained areas were frequently located at the tumor front, satellite nodules, and in lymphovascular spaces (Figure S2). For the clinicopathological correlation, both MYST4 1+ HCCs (*P*=0.0077; **Figure 1C**) and MYST4 3+ HCCs (*P*=0.0038; **Figure 1D**) were associated with worse 5-year overall survival compared to MYST4 non-expressing HCCs. Therefore, our results indicated that the expression level of MYST4 is an important clinicopathological parameter which is correlated with HG morphology and associated with reduced survival.

Comparison of MYST4 levels among different human cancer cell lines and verification of the knockdown efficiency in three selected high MYST4-expressing cell lines

To select cell lines for the further functional study of MYST4, we next examined the expression level of MYST4 in human cancer cell lines from the ovary, breast, liver, colon, lung, tongue, stomach, and urinary bladder by qRT-PCR. Higher levels of MYST4 were detected in OCs, breast carcinomas and HCCs. As shown in **Figure 2A**, the main cell lines studied included two OC cell lines (A2780 and OVCAR3), eight breast cancer cell lines (SKBR3, MB361, HCC193, HBL435, MB468, MB435, T47D, and THME), and ten liver cancer cell lines (SKHEP1, HEP3B, MAHLA, Huh7, VGH, HCC36, PLC5, HA-59T, HEPG2, and Huh7VG) (**Figure 2A**). Based on the screening results, we selected three cell lines (A2780, SKBR3, and Huh7) for further MYST4-knockdown and functional investigation.

MYST4-knockdown were performed in A2780, SKBR3, and Huh7 cells using five shRNAs clones (clones 21, 48, 49, 51, and 63), and two (shMYST4-48 and shMYST4-51) were found to

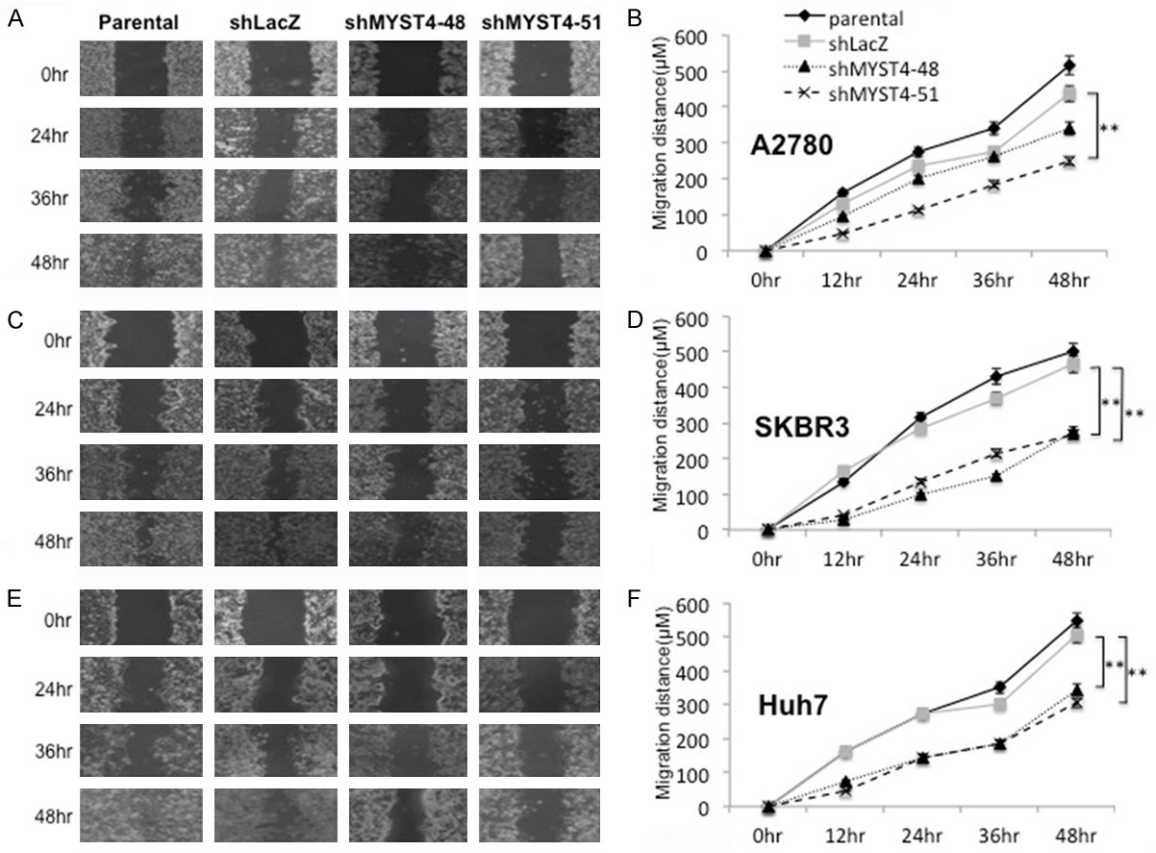

Figure 4. Knockdown of MYST4 suppresses cell migration. The cell migration ability was assessed using a monolayer wound-healing assay. Representative photos and charts of cell migration distances (μM) at 0, 24, 36, and 48 h are shown in (A, B) A2780, (C, D) SKBR3, and (E, F) Huh7 cells. Knockdown clones shMYST4-48 and -51 showed significantly suppressed migration activities compared to the control (sh*LacZ*) and parental cells. Data are presented as the mean ± SD of three independent experiments. ***P*<0.01.

have a significant silencing effect compared to the mock control (shLacZ) and parental cells (*P*<0.05; *P*<0.01; **Figure 2B**). Among them, clone shMYST4-51 was the most effective for MYST4 silencing.

MYST4 silencing significantly suppressed cell proliferation, cell cycle progression, and cell migration in vitro

The rearrangement of MYST4 was reported to be associated with several cancers [25, 29]; however, the fundamental mechanisms remain controversial. To investigate the role of MYST4 in human solid tumors, we examined whether MYST4 affects cell proliferation using MYST4-knockdown in selected cancer lines. Cells were seeded in 12-well plates and incubated with appropriate culture conditions; cell numbers were then counted each day for 5 consecutive days. As shown in **Figure 2**, both MYST4-knockdown clones (shMYST4-48 and shMYST4-51) in all three cancer cell lines A2780 (OC; *P*<0.05; **Figure 2C** upper panel), SKBR3 (breast cancer; *P*<0.05; **Figure 2C** middle panel), and Huh7 (HCC; *P*<0.05; **Figure 2C** lower panel) showed significantly reduced cell proliferation activities compared to the mock control (sh*LacZ*) and parental cells (**Figure 2C**).

In addition, the effect of MYST4 on cell cycle progression was also investigated using a flow cytometric analysis. Both knockdown clones (shMYST4-48 and shMYST4-51) showed higher cell numbers in the G_0/G_1 phase and lower cell numbers in the G_2/M phase compared to the mock control (sh*LacZ*) and parental cells in A2780 (*P*<0.01; **Figure 3A**), SKBR3 (*P*<0.01; **Figure 3B**), and Huh7 cells (*P*<0.01; **Figure 3C**) (**Figure 3**). These data indicated that silencing MYST4 forces cell cycle arrest at G_2/M phase, resulting in reduced cell proliferation activities.

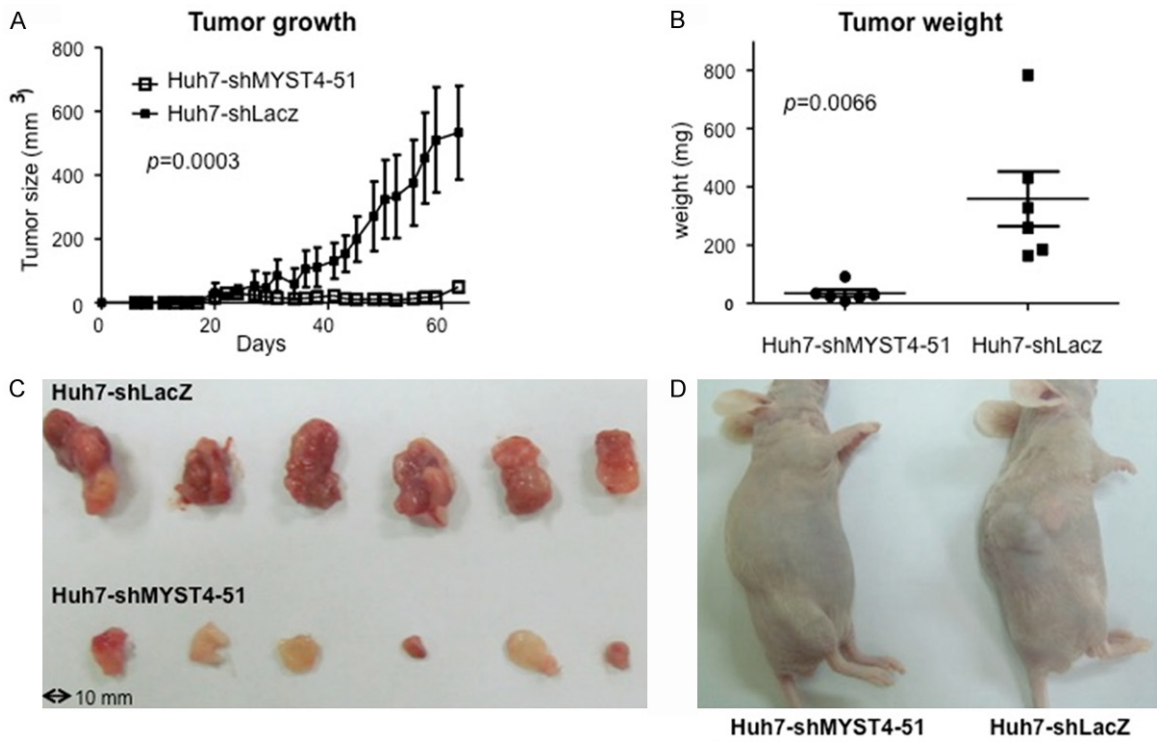

Figure 5. Silencing of MYST4 reduces tumor cell growth in vivo. MYST4-silenced Huh7 cells xenografted into NOD/SCID mice were allowed to grow for 63 days. A and D. Mean tumor sizes of the two groups (n=6 per group) significantly differed (mm^3, ***P=0.0003). B and C. Tumors dissected from the mock control (sh*LacZ*) transfected Huh7 xenografts appeared to be larger (scale bar is 10 mm) and heavier (mg, ***P=0.0066) than the knockdown cell Huh7-shMYST4-51 xenografts.

To further investigate the roles of MYST4 in tumor progression and the cell migration ability, cell migration was observed at 12, 24, 36, and 48 h following the creation of a scratch wound. As revealed by this wound-healing assay, cells transfected with the knockdown clones shMYST4-48 and shMYST4-51 migrated significantly more slowly during an incubation period of 36~48 h in A2780 (P<0.01; **Figure 4A**, **4B**), SKBR3 (P<0.01; **Figure 4C**, **4D**), and Huh7 cells (P<0.01; **Figure 4E**, **4F**) compared to the mock control (sh*LacZ*) and parental cells.

Identification of potentially MYST4 regulated genes by microarray study

Through a microarray analysis to elucidate the mechanisms, we identified 4353 genes with more than a 2-fold change in three cancer cell lines (A2780, SKBR3 and Huh7), among which 32 genes had reduced mRNA expression in MYST4-knockdown cell lines (Figure S3). Among these genes, six had been reported to be involved in regulating tumors, including cathepsin Z (CTSZ) [30], NAD-dependent deacetylase sirtuin-2 (SIRT2) [31], solute carrier family 39 member 14 (SLC39A14; also known as ZIP14) [32], metastasis-associated lung adenocarcinoma transcript 1 (MALAT1) [33], Mps one binder kinase activator-like 2B (yeast) (MOBKL2B; also known as MOB3B) [34], and homeobox B8 (HOXB8) [35] (Figure S3).

MYST4-knockdown limits the tumor growth ability in mouse xenografts

We further investigated the effect of MYST4 on tumor growth *in vivo* using tumor xenografts in mice. The MYST4 shRNA-knockdown clone (shMYST4-51) and mock control sh*LacZ* Huh7 cells were subcutaneously injected into female athymic *nu/nu* mice (n=6 mice per group; **Figure 5**) at 10^7 cells per mouse. After 9 weeks, tumors dissected from mock-transfected (sh*LacZ*) Huh7 cells were used for comparison, and these showed a larger tumor size than tumors from mice treated with shMYST4-51-transfected Huh7 cells (P=0.0003; **Figure 5A**, **5D**). Photos of individual tumor sizes from each xenograft mouse group are shown (scale bar is

10 mm; **Figure 5C**) and weighed (in mg; *P*=0.0066; **Figure 5D**). Tumor sizes and weights showed significant reductions in shMYST4-51-transfected Huh7 xenograft mice. The health status of the tested mice was monitored throughout the experiments by a health surveillance program according to ACCMU guidelines. When sacrificed, the mice were found free of inflammation and SPF infection.

Discussion

Epigenetic regulation of gene expression through histone modifications is a major process controlling cell growth and development. Studies have shown that MYST4, one of the HATs, plays important roles in chromatin remodeling and is associated with a variety of cell functions, including tumorigenesis [36, 37]. We identified that overexpression of the *MYST4* gene is preferentially associated with HGSC type in OCs and was correlated with diminished survival of OC and HCC patients (**Figures 1**, S2). To our knowledge, this is the first study investigating the correlation of MYST4 with clinical significance in human solid tumors.

In this study, we screened several cancer cell lines from three different solid tumors including OCs, breast cancers, and HCCs and selected relatively high-level MYST4-expressing cell lines for further investigation using a MYST4-silencing strategy. Functional studies of MYST4, as shown in **Figures 2**-**4**, demonstrated that knockdown of MYST4 significantly reduced cell proliferation and migration due to an accumulation of cells in the G_2/M phase during cell-cycle progression. Our extensive *in vitro* and *in vivo* studies in cancer cell lines and mice consistently revealed that MYST4 regulates cell proliferation, and hence might be involved in carcinogenesis or tumor progression of solid tumors. Similarly, recent studies revealed that epigenetic regulation of other HAT family members, CREB-binding protein (CBP) and p300, are also key regulators of cell differentiation and carcinogenesis in OC [38] due to their HAT activities, whereas a p300/CBP inhibitor exhibited antiproliferative and proapoptotic properties in several types of cancer cells, including leukemia, melanoma, pancreatic, and prostate cancers [39-42]. Moreover, BRCA2, a prognostic marker for breast cancer, was reported to specifically interact with the HAT p300/CBP-associated factor (P/CAF) [43, 44] due to its HAT activity. Thus, BRCA2 recruits P/CAF and mediates the association and acetylation of the BubR1: BRCA2 complex for the proper control of mitosis [45].

As for the association of HATs to HCC, although the mechanism is still unclear, one recent study found that HAT1 might act as an oncogenic protein that promotes cell proliferation and induces cisplatin resistance in HCC [46]. Our results also suggest that knockdown of MYST4 reduced Huh7 cell proliferation and migration and caused G_2/M arrest *in vitro*. Furthermore, silencing of MYST4 in Huh7 cells significantly suppressed tumor growth in a mice xenograft model (**Figure 5**) *in vivo*. Investigations of HATs in tumorigenesis showed that MYST4 specifically regulates the RAS/mitogen-activated protein kinase (MAPK) signaling pathway via H3 acetylation *in vivo* and *in vitro* in humans and mice [17]. Besides, P300/CBP-associated factor (PCAF), which serves as a prognostic marker, was downregulated in HCC tissues and showed PCAF-induced autophagy in HCC cells through the inhibition of the Akt/mammalian target of rapamycin (mTOR) pathway [47, 48], which may serve as a therapeutic candidate for HCC treatment. Moreover, accumulating evidence indicates that CBP/p300 plays an important role in the cancer phenotype. CBP/p300 promoted cancer progression in colon cancer cell lines with microsatellite instability [49]. P300 regulated p53-dependent apoptosis after DNA damage [50] and disrupted the p300-promoted epithelial to mesenchymal transition (EMT) thus causing an aggressive cancer phenotype in colon cancer [51]. Our microarray study expands the spectrum of interacting genes that might play important roles in MYST4 overexpressing tumors and deserves further investigation.

Histone acetylation relaxes the normally tight supercoiling of chromatin, which is associated with transcriptional activation of genes that regulate cell cycle progression, DNA replication, and the apoptotic response to DNA damage [52]. HATs, such as MYST4, promote transcription by functioning as transcriptional adaptors between enhancer-bound transcription factors and the basal transcription apparatus, as well as by acetylating more than 70 different proteins. Our results demonstrate that MYST4 is involved in solid tumor progression, including OCs, breast cancers, and HCCs and was signifi-

cantly correlated with the survival of clinical patients. In addition, the knockdown of MYST4 significantly diminished cell proliferation and migration due to accumulating cells in the G_2/M stage *in vitro*. In the *in vivo* tumor xenograft mice model, the silencing of MYST4 in Huh7 cells significantly suppressed tumor growth by inhibiting MYST4 HAT activity. Taken together, our results suggest that targeting MYST4 may provide a novel therapeutic strategy for treating human solid tumors.

Conclusions

We conclude that MYST4, one of the histone acetyltransferases (HATs), is involved in cancer progression and contributes to more aggressive behavior in human solid tumors, including ovarian carcinomas (OCs), breast carcinomas, and hepatocellular carcinomas (HCCs). Therefore, targeting MYST4 represents an appealing strategy for effective treatment of advanced solid tumors overexpressing MYST4.

Acknowledgements

We thank past and present laboratory members for their inspired work and stimulating discussions. The study of human subjects was approved by the Ethics Committee and Review Board at National Taiwan University Hospital (approval no.: 201112064RIC). The animal study was approved by the Institute Animal Care and Use Committee (IACUC) of CMU (101-24-N). This work was supported by a grant (MOST101-2320-B-002-016-MY3) from the Ministry of Science and Technology (MOST), Taiwan to TLM and a grant DMR-105-064 from China Medical University Hospital (CMUH), Taichung, Taiwan to CYYC.

Disclosure of conflict of interest

None.

Abbreviations

HATs, histone acetyltransferases; SAGE, serial analysis of gene expression; PHD, plant homeodomain-linked; OCs, ovarian carcinomas; HCCs, hepatocellular carcinomas; MYST4 (MORF), MOZ-related factor; EM, endometrioid; CCC, clear cell carcinoma; HGSCs, ovarian HG serous carcinomas; IHC, immunohistochemistry; DMEM, Dulbecco's modified Eagle's medium; PBS, phosphate-buffered saline; CBP, CREB-binding protein (CBP); P/CAF, p300/CBP-associated factor; mTOR, mammalian target of rapamycin; ACCMU, the Animal Center at China Medical University.

Address correspondence to: Dr. Tsui-Lien Mao, Department of Pathology, National Taiwan University Hospital, No. 7 Chung-San South Road, Taipei 100, Taiwan. Tel: +886-2-23123456 Ext. 65453; Fax: +886-2-23934172; E-mail: tlmao@ntu.edu.tw

References

[1] Egger G, Liang G, Aparicio A, Jones PA. Epigenetics in human disease and prospects for epigenetic therapy. Nature 2004; 429: 457-463.

[2] Jaenisch R and Bird A. Epigenetic regulation of gene expression: how the genome integrates intrinsic and environmental signals. Nat Genet 2003; 33 Suppl: 245-254.

[3] Lee KK and Workman JL. Histone acetyltransferase complexes: one size doesn't fit all. Nat Rev Mol Cell Biol 2007; 8: 284-295.

[4] Yang XJ. The diverse superfamily of lysine acetyltransferases and their roles in leukemia and other diseases. Nucleic Acids Res 2004; 32: 959-976.

[5] Khorasanizadeh S. The nucleosome: from genomic organization to genomic regulation. Cell 2004; 116: 259-272.

[6] Kouzarides T. Chromatin modifications and their function. Cell 2007; 128: 693-705.

[7] Champagne N, Pelletier N and Yang XJ. The monocytic leukemia zinc finger protein MOZ is a histone acetyltransferase. Oncogene 2001; 20: 404-409.

[8] Champagne N, Bertos NR, Pelletier N, Wang AH, Vezmar M, Yang Y, Heng HH, Yang XJ. Identification of a human histone acetyltransferase related to monocytic leukemia zinc finger protein. J Biol Chem 1999; 274: 28528-36.

[9] Campeau PM, Lu JT, Dawson BC, Fokkema IF, Robertson SP, Gibbs RA, Lee BH. The KAT6B-related disorders genitopatellar syndrome and Ohdo/SBBYS syndrome have distinct clinical features reflecting distinct molecular mechanisms. Hum Mutat 2012; 33: 1520-5.

[10] Borrow J, Stanton VP Jr, Andresen JM, Becher R, Behm FG, Chaganti RS, Civin CI, Disteche C, Dubé I, Frischauf AM, Horsman D, Mitelman F, Volinia S, Watmore AE, Housman DE. The translocation t(8;16)(p11;p13) of acute myeloid leukaemia fuses a putative acetyltransferase to the CREB-binding protein. Nat Genet 1996; 14: 33-41.

[11] Takechi S and Nakayama T. Sas3 is a histone acetyltransferase and requires a zinc finger motif. Biochem Biophys Res Commun 1999; 266: 405-10.

[12] Ran Q and Pereira-Smith OM. Identification of an alternatively spliced form of the Tat interactive protein (Tip60), Tip60 (beta). Gene 2000; 258: 141-6.
[13] Wang J, Rao S, Chu J, Shen X, Levasseur DN, Theunissen TW, Orkin SH. A protein interaction network for pluripotency of embryonic stem cells. Nature 2006; 127: 1137-1150.
[14] Mendjan S, Taipale M, Kind J, Holz H, Gebhardt P, Schelder M, Vermeulen M, Buscaino A, Duncan K, Mueller J, Wilm M, Stunnenberg HG, Saumweber H, Akhtar A. Nuclear pore components are involved in the transcriptional regulation of dosage compensation in drosophila. Mol Cell 2006; 21: 811-23.
[15] Sykes SM, Mellert HS, Holbert MA, Li K, Marmorstein R, Lane WS, McMahon SB. Acetylation of the p53 DNA-binding domain regulates apoptosis induction. Mol Cell 2006; 24: 841-851.
[16] Tang Y, Luo J, Zhang W, Gu W. Tip60-dependent acetylation of p53 modulates the decision between cell-cycle arrest and apoptosis. Mol Cell 2006; 24: 827-839.
[17] Kraft M, Cirstea IC, Voss AK, Thomas T, Goehring I, Sheikh BN, Gordon L, Scott H, Smyth GK, Ahmadian MR, Trautmann U, Zenker M, Tartaglia M, Ekici A, Reis A, Dörr HG, Rauch A, Thiel CT. Disruption of the histone acetyltransferase MYST4 leads to a noonan syndrome-like phenotype and hyperactivated MAPK signaling in humans and mice. J Clin Invest 2011; 121: 3479-3491.
[18] Szakszon K, Salpietro C, Kakar N, Knegt AC, Oláh É, Dallapiccola B, Borck G. De novo mutations of the gene encoding the histone acetyltransferase KAT6B in two patients with Say-Barber/Biesecker/Young-Simpson syndrome. Am J Med Genet A 2013; 161A: 884-888.
[19] Clayton-Smith J, O'Sullivan J, Daly S, Bhaskar S, Day R, Anderson B, Voss AK, Thomas T, Biesecker LG, Smith P, Fryer A, Chandler KE, Kerr B, Tassabehji M, Lynch SA, Krajewska-Walasek M, McKee S, Smith J, Sweeney E, Mansour S, Mohammed S, Donnai D, Black G. Whole-exome-sequencing identifies mutations in histone acetyltransferase gene KAT6B in individuals with the Say-Barber-Biesecker variant of ohdo syndrome. Am J Hum Genet 2011; 89: 675-681.
[20] Simpson MA, Deshpande C, Dafou D, Vissers LE, Woollard WJ, Holder SE, Gillessen-Kaesbach G, Derks R, White SM, Cohen-Snuijf R, Kant SG, Hoefsloot LH, Reardon W, Brunner HG, Bongers EM, Trembath RC. De novo mutations of the gene encoding the histone acetyltransferase KAT6B cause genitopatellar syndrome. Am J Hum Genet 2012; 90: 290-294.
[21] Campeau PM, Kim JC, Lu JT, Schwartzentruber JA, Abdul-Rahman OA, Schlaubitz S, Murdock DM, Jiang MM, Lammer EJ, Enns GM, Rhead WJ, Rowland J, Robertson SP, Cormier-Daire V, Bainbridge MN, Yang XJ, Gingras MC, Gibbs RA, Rosenblatt DS, Majewski J, Lee BH. Mutations in KAT6B, encoding a histone acetyltransferase, cause genitopatellar syndrome. Am J Hum Genet 2012; 90: 282-9.
[22] Yu HC, Geiger EA, Medne L, Zackai EH, Shaikh TH. An individual with blepharophimosis-ptosis-epicanthus inversus syndrome (BPES) and additional features expands the phenotype associated with mutations in KAT6B. Am J Med Genet A 2014; 164A: 950-957.
[23] Panagopoulos I, Fioretos T, Isaksson M, Samuelsson U, Billström R, Strömbeck B, Mitelman F, Johansson B. Fusion of the MORF and CBP genes in acute myeloid leukemia with the t(10;16)(q22;p13). Hum Mol Genet 2001; 10: 395-404.
[24] Kojima K, Kaneda K, Yoshida C, Dansako H, Fujii N, Yano T, Shinagawa K, Yasukawa M, Fujita S, Tanimoto M. A novel fusion variant of the MORF and CBP genes detected in therapy-related myelodysplastic syndrome with t(10;16)(q22;p13). Br J Haematol 2003; 120: 271-273.
[25] Moore SD, Herrick SR, Ince TA, Kleinman MS, Dal Cin P, Morton CC, Quade BJ. Uterine leiomyomata with t(10;17) disrupt the histone acetyltransferase MORF. Cancer Res 2004; 64: 5570-5577.
[26] Panagopoulos I, Gorunova L, Bjerkehagen B, Heim S. Novel KAT6B-KANSL1 fusion gene identified by RNA sequencing in retroperitoneal leiomyoma with t(10;17)(q22;q21). PLoS One 2015; 10: e0117010.
[27] Lynch H, Wen H, Kim YC, Snyder C, Kinarsky Y, Chen PX, Xiao F, Goldgar D, Cowan KH, Wang SM. Can unknown predisposition in familial breast cancer be family-specific? Breast J 2013; 19: 520-528.
[28] Grasso CS, Wu YM, Robinson DR, Cao X, Dhanasekaran SM, Khan AP, Quist MJ, Jing X, Lonigro RJ, Brenner JC, Asangani IA, Ateeq B, Chun SY, Siddiqui J, Sam L, Anstett M, Mehra R, Prensner JR, Palanisamy N, Ryslik GA, Vandin F, Raphael BJ, Kunju LP, Rhodes DR, Pienta KJ, Chinnaiyan AM, Tomlins SA. The mutational landscape of lethal castration-resistant prostate cancer. Nature 2012; 487: 239-243.
[29] Yang XJ, Ullah M. MOZ and MORF, two large MYSTic HATs in normal and cancer stem cells. Oncogene 2007; 26: 5408-5419.
[30] Pungercar J, Ivanovski G. Identification and molecular cloning of cathepsin p, a novel human putative cysteine protease of the papain family. Pflugers Arch 2000; 439 Suppl: R116-118.
[31] Serrano L, Martínez-Redondo P, Marazuela-Duque A, Vazquez BN, Dooley SJ, Voigt P, Beck

DB, Kane-Goldsmith N, Tong Q, Rabanal RM, Fondevila D, Muñoz P, Krüger M, Tischfield JA, Vaquero A. The tumor suppressor SirT2 regulates cell cycle progression and genome stability by modulating the mitotic deposition of H4K20 methylation. Genes Dev 2013; 27: 639-653.

[32] Taylor KM, Nicholson RI. The LZT proteins; the LIV-1 subfamily of zinc transporters. Biochim Biophys Acta 2003; 1611: 16-30.

[33] Gutschner T, Hämmerle M, Eissmann M, Hsu J, Kim Y, Hung G, Revenko A, Arun G, Stentrup M, Gross M, Zörnig M, MacLeod AR, Spector DL, Diederichs S. The noncoding RNA MALAT1 is a critical regulator of the metastasis phenotype of lung cancer cells. Cancer Res 2013; 73: 1180-1189.

[34] Hartmann EM, Campo E, Wright G, Lenz G, Salaverria I, Jares P, Xiao W, Braziel RM, Rimsza LM, Chan WC, Weisenburger DD, Delabie J, Jaffe ES, Gascoyne RD, Dave SS, Mueller-Hermelink HK, Staudt LM, Ott G, Beà S, Rosenwald A. Pathway discovery in mantle cell lymphoma by integrated analysis of high-resolution gene expression and copy number profiling. Blood 2010; 116: 953-961.

[35] Peverali FA, D'Esposito M, Acampora D, Bunone G, Negri M, Faiella A, Stornaiuolo A, Pannese M, Migliaccio E, Simeone A, et al. Expression of HOX homeogenes in human neuroblastoma cell culture lines. Differentiation 1990; 45: 61-69.

[36] Dou Y, Milne TA, Tackett AJ, Smith ER, Fukuda A, Wysocka J, Allis CD, Chait BT, Hess JL, Roeder RG. Physical association and coordinate function of the H3 K4 methyltransferase MLL1 and the H4 K16 acetyltransferase MOF. Cell 2005; 121: 873-885.

[37] Yang XJ. MOZ and MORF acetyltransferases: molecular interaction, animal development and human disease. Biochim Biophys Acta 2015; 1853: 1818-1826.

[38] Gatla HR, Zou Y, Uddin MM, Vancurova I. Epigenetic regulation of interleukin-8 expression by class I HDAC and CBP in ovarian cancer cells. Oncotarget 2017; 8: 70798-70810.

[39] Bowers EM, Yan G, Mukherjee C, Orry A, Wang L, Holbert MA, Crump NT, Hazzalin CA, Liszczak G, Yuan H, Larocca C, Saldanha SA, Abagyan R, Sun Y, Meyers DJ, Marmorstein R, Mahadevan LC, Alani RM, Cole PA. Virtual ligand screening of the p300/CBP histone acetyltransferase: identification of a selective small molecule inhibitor. Chem Biol 2010; 17: 471-482.

[40] Santer FR, Höschele PP, Oh SJ, Erb HH, Bouchal J, Cavarretta IT, Parson W, Meyers DJ, Cole PA, Culig Z. Inhibition of the acetyltransferases p300 and CBP reveals a targetable function for p300 in the survival and invasion pathways of prostate cancer cell lines. Mol Cancer Ther 2011; 10: 1644-1655.

[41] Yan G, Eller MS, Elm C, Larocca CA, Ryu B, Panova IP, Dancy BM, Bowers EM, Meyers D, Lareau L, Cole PA, Taverna SD, Alani RM. Selective inhibition of p300 HAT blocks cell cycle progression, induces cellular senescence, and inhibits the DNA damage response in melanoma cells. J Invest Dermatol 2013; 133: 2444-2452.

[42] Ono H, Basson MD, Ito H. P300 inhibition enhances gemcitabine-induced apoptosis of pancreatic cancer. Oncotarget 2016; 7: 51301-51310.

[43] Fuks F, Milner J, Kouzarides T. BRCA2 associates with acetyltransferase activity when bound to P/CAF. Oncogene 1998; 17: 2531-2534.

[44] Kwon WS, Rha SY, Jeung HC, Kim TS, Chung HC. Modulation of HAT activity by the BRCA2 N372H variation is a novel mechanism of paclitaxel resistance in breast cancer cell lines. Biochem Pharmacol 2017; 138: 163-173.

[45] Choi E, Choe H, Min J, Choi JY, Kim J, Lee H. BubR1 acetylation at prometaphase is required for modulating APC/C activity and timing of mitosis. EMBO J 2009; 28: 2077-2089.

[46] Jin X, Tian S, Li P. Histone acetyltransferase 1 promotes cell proliferation and induces cisplatin resistance in hepatocellular carcinoma. Oncol Res 2017; 25: 939-946.

[47] Liu YL, Yang PM, Shun CT, Wu MS, Weng JR, Chen CC. Autophagy potentiates the anti-cancer effects of the histone deacetylase inhibitors in hepatocellular carcinoma. Autophagy 2010; 6: 1057-65.

[48] Jia YL, Xu M, Dou CW, Liu ZK, Xue YM, Yao BW, Ding LL, Tu KS, Zheng X, Liu QG. P300/CBP-associated factor (PCAF) inhibits the growth of hepatocellular carcinoma by promoting cell autophagy. Cell Death Dis 2016; 7: e2400.

[49] Ionov Y, Matsui S, Cowell JK. A role for p300/CREB binding protein genes in promoting cancer progression in colon cancer cell lines with microsatellite instability. Proc Natl Acad Sci U S A 2004; 101: 1273-1278.

[50] Iyer NG, Chin SF, Ozdag H, Daigo Y, Hu DE, Cariati M, Brindle K, Aparicio S, Caldas C. p300 regulates p53-dependent apoptosis after DNA damage in colorectal cancer cells by modulation of PUMA/p21 levels. Proc Natl Acad Sci U S A 2004; 101: 7386-7391.

[51] Krubasik D, Iyer NG, English WR, Ahmed AA, Vias M, Roskelley C, Brenton JD, Caldas C, Murphy G. Absence of p300 induces cellular phenotypic changes characteristic of epithelial to mesenchyme transition. Br J Cancer 2006; 94: 1326-1332.

[52] Reed NA, Cai D, Blasius TL, Jih GT, Meyhofer E, Gaertig J, Verhey KJ. Microtubule acetylation promotes kinesin-1 binding and transport. Curr Biol 2006; 16: 2166-2172.

MYST4 overexpression in human solid tumors

Total Tags:		49394	51893	61083	55418	54920	58868	17353	43891	57725	36813
Normalization:		2.02	1.93	1.64	1.80	1.82	1.70	5.76	2.28	1.73	2.72
Gene Name	**Mean**	**HOSE4**	**IOSE29**	**ML10**	**JH514**	**JH648**	**OVCA3**	**OC14**	**OVT6**	**OVT7**	**OVT8**
AIRE	1.1	0.0	0.0	3.3	0.0	0.0	0.0	5.8	4.6	0.0	0.0
ASH1L	0.0	0.0	0.0	0.0	0.0	0.0	0.0	0.0	2.3	0.0	0.0
ASXL1	6.6	2.0	9.6	8.2	7.2	9.1	5.1	17.3	6.8	12.1	0.0
BAZ1A	1.2	0.0	1.9	1.6	0.0	1.8	1.7	0.0	2.3	3.5	0.0
BAZ1B	12.7	2.0	21.2	14.7	7.2	5.5	15.3	5.8	9.1	6.9	8.1
BAZ2B	4.7	4.0	1.9	8.2	3.6	10.9	1.7	0.0	13.7	3.5	10.9
BHC80	17.7	8.1	27.0	18.0	7.2	9.1	20.4	28.8	9.1	26.0	19.0
BRPF1	0.0	0.0	0.0	0.0	1.8	1.8	0.0	5.8	0.0	1.7	2.7
BRPF3	3.2	4.0	3.9	1.6	1.8	1.8	1.7	5.8	2.3	0.0	2.7
C20orf104	6.3	0.0	5.8	13.1	1.8	9.1	3.4	5.8	2.3	10.4	0.0
CGI-72	14.3	10.1	11.6	21.3	19.8	14.6	11.9	17.3	9.1	32.9	16.3
CHD3	4.2	2.0	5.8	4.9	1.8	5.5	10.2	5.8	20.5	5.2	8.1
CHD4	22.1	4.0	32.8	29.5	23.5	23.7	42.5	34.6	34.2	26.0	29.9
CHD5	0.6	0.0	1.9	0.0	0.0	1.8	3.4	0.0	2.3	0.0	2.7
CXXC1	1.3	2.0	1.9	0.0	5.4	3.6	10.2	0.0	2.3	8.7	2.7
DATF1	1.2	0.0	1.9	1.6	0.0	7.3	10.2	0.0	2.3	5.2	2.7
DPF1	2.5	0.0	5.8	1.6	0.0	0.0	1.7	5.8	0.0	0.0	0.0
DPF2	5.4	4.0	3.9	8.2	5.4	5.5	0.0	0.0	4.6	1.7	8.1
FALZ	3.8	0.0	9.6	1.6	0.0	0.0	1.7	5.8	11.4	1.7	0.0
FBXL10	2.4	4.0	0.0	3.3	3.6	0.0	6.8	17.3	6.8	5.2	8.1
FBXL11	14.5	8.1	17.3	18.0	0.0	12.7	13.6	23.1	22.8	17.3	13.6
HBXAP	12.8	8.1	17.3	13.1	9.0	10.9	49.3	17.3	15.9	6.9	13.6
HOZFP	1.7	0.0	1.9	3.3	1.8	3.6	1.7	0.0	0.0	12.1	2.7
ING1	0.6	0.0	1.9	0.0	0.0	3.6	0.0	5.8	4.6	1.7	5.4
ING1L	1.3	0.0	3.9	0.0	0.0	1.8	0.0	0.0	2.3	3.5	0.0
ING3	1.2	0.0	1.9	1.6	1.8	3.6	8.5	5.8	9.1	6.9	8.1
ING4	2.0	6.1	0.0	0.0	3.6	1.8	3.4	0.0	6.8	0.0	8.1
ING5	9.9	20.2	7.7	1.6	14.4	5.5	0.0	0.0	0.0	0.0	2.7
JARID1A	19.5	14.2	23.1	21.3	12.6	5.5	1.7	11.5	11.4	15.6	8.1
JARID1B	3.0	0.0	5.8	3.3	1.8	3.6	6.8	0.0	4.6	0.0	8.1
JARID1C	7.7	10.1	9.6	3.3	0.0	12.7	15.3	0.0	0.0	0.0	0.0
JARID1D	0.0	0.0	0.0	0.0	1.8	0.0	0.0	0.0	0.0	0.0	2.7
JMJD2A	5.3	0.0	7.7	8.2	3.6	3.6	6.8	11.5	6.8	3.5	5.4
JMJD2B	8.1	4.0	15.4	4.9	7.2	12.7	3.4	11.5	13.7	8.7	2.7
JMJD2C	5.1	8.1	3.9	3.3	9.0	7.3	1.7	17.3	11.4	3.5	8.1
KIAA1333	4.7	2.0	3.9	8.2	1.8	1.8	10.2	17.3	11.4	3.5	5.4
KIAA1542	4.9	4.0	5.8	4.9	1.8	0.0	5.1	5.8	2.3	5.2	2.7
KIAA1718	3.5	2.0	1.9	6.5	3.6	5.5	5.1	0.0	0.0	5.2	8.1
LOC57117	0.0	0.0	0.0	0.0	0.0	0.0	1.7	0.0	0.0	0.0	0.0
M96	4.4	2.0	9.6	1.6	1.8	1.8	3.4	11.5	4.6	3.5	5.4
MLL	12.2	4.0	21.2	11.5	16.2	14.6	10.2	5.8	15.9	8.7	0.0
MLL2	3.0	0.0	5.8	3.3	0.0	0.0	3.4	23.1	0.0	0.0	0.0
MLL3	4.2	2.0	5.8	4.9	9.0	5.5	8.5	5.8	6.8	12.1	0.0
MLL4	3.1	2.0	3.9	3.3	3.6	3.6	8.5	11.5	4.6	3.5	10.9
MLL5	8.8	12.1	7.7	6.5	9.0	10.9	5.1	0.0	4.6	6.9	5.4
MLLT10	0.0	0.0	0.0	0.0	0.0	1.8	0.0	0.0	0.0	0.0	0.0
MLLT6	3.0	2.0	1.9	4.9	7.2	12.7	13.6	5.8	6.8	3.5	21.7
MYST3	4.7	0.0	5.8	8.2	1.8	3.6	8.5	17.3	0.0	3.5	2.7
MYST4	10.1	2.0	13.5	14.7	3.6	21.8	20.4	40.3	18.2	13.9	21.7
NFX1	6.6	4.0	5.8	9.8	1.8	3.6	1.7	17.3	2.3	0.0	2.7
NSD1	2.2	0.0	0.0	6.5	1.8	1.8	0.0	5.8	2.3	0.0	0.0
PHF1	5.9	2.0	5.8	9.8	3.6	3.6	1.7	0.0	4.6	5.2	0.0
PHF10	4.6	10.1	1.9	1.6	0.0	1.8	1.7	5.8	2.3	3.5	2.7
PHF11	3.3	8.1	1.9	0.0	5.4	1.8	1.7	5.8	4.6	3.5	10.9
PHF12	5.3	10.1	5.8	0.0	12.6	1.8	10.2	5.8	2.3	0.0	8.1
PHF13	2.6	2.0	5.8	0.0	0.0	0.0	6.8	5.8	6.8	1.7	2.7
PHF15	8.5	10.1	3.9	11.5	1.8	0.0	3.4	5.8	6.8	12.1	5.4
PHF16	10.0	16.2	3.9	9.8	12.6	12.7	22.1	34.6	2.3	12.1	13.6
PHF17	4.0	2.0	1.9	8.2	1.8	3.6	5.1	17.3	6.8	1.7	2.7
PHF19	3.6	2.0	3.9	4.9	3.6	1.8	1.7	0.0	0.0	1.7	0.0
PHF2	3.5	0.0	3.9	6.5	1.8	10.9	1.7	5.8	2.3	5.2	2.7
PHF3	57.5	70.9	44.3	57.3	93.8	52.8	66.2	28.8	45.6	69.3	35.3
PHF5A	2.2	0.0	0.0	6.5	7.2	3.6	1.7	0.0	2.3	3.5	2.7
PHF6	4.3	4.0	3.9	4.9	12.6	1.8	5.1	17.3	4.6	12.1	2.7
PHF7	1.1	0.0	0.0	3.3	1.8	0.0	1.7	0.0	2.3	3.5	2.7
PHF8	1.8	2.0	0.0	3.3	5.4	1.8	0.0	0.0	2.3	3.5	2.7
PRKCBP1	3.6	2.0	3.9	4.9	10.8	9.1	6.8	5.8	13.7	12.1	8.1
PYGO2	3.9	2.0	9.6	0.0	1.8	1.8	10.2	0.0	0.0	1.7	2.7
RAI1	2.9	0.0	3.9	4.9	0.0	0.0	1.7	0.0	0.0	1.7	0.0
SHPRH	3.5	2.0	1.9	6.5	9.0	3.6	1.7	17.3	2.3	1.7	5.4
SP100	2.4	4.0	0.0	3.3	7.2	10.9	6.8	0.0	4.6	5.2	8.1
SP140	1.3	0.0	3.9	0.0	1.8	1.8	0.0	0.0	0.0	0.0	0.0
TCF19	1.2	0.0	1.9	1.6	5.4	0.0	3.4	0.0	0.0	0.0	0.0
TIF1	4.8	2.0	5.8	6.5	1.8	10.9	1.7	0.0	4.6	6.9	5.4
TRIM28	29.6	14.2	38.5	36.0	23.5	16.4	39.1	17.3	9.1	19.1	19.0
TRIM33	2.3	0.0	1.9	4.9	0.0	3.6	3.4	5.8	11.4	3.5	8.1
UHRF1	5.4	0.0	9.6	6.5	7.2	0.0	1.7	5.8	2.3	1.7	0.0
UHRF2	3.2	0.0	9.6	0.0	1.8	1.8	0.0	11.5	13.7	5.2	2.7
WHSC1	8.2	0.0	11.6	13.1	10.8	3.6	22.1	5.8	4.6	6.9	10.9
WHSC1L1	2.3	0.0	1.9	4.9	0.0	0.0	0.0	11.5	4.6	3.5	0.0

Figure S1. MYST4 is overexpressed in ovarian high-grade serous carcinoma using a SAGE. The SAGE was performed using PHD domain containing genes in ovarian cancer cell lines and tumor tissues. A high level of MYST4 expression was found in OC14 cells.

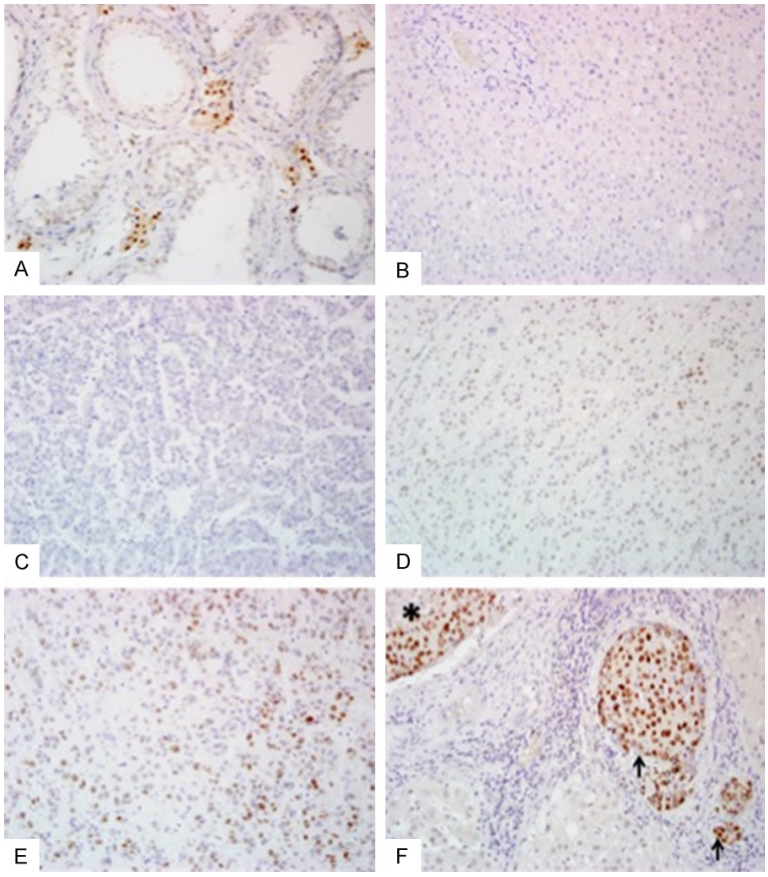

Figure S2. MYST4 expression levels in hepatocellular carcinoma (HCC) and normal tissues using IHC staining. Tissue sections were stained with a MYST4 antibody (A). Control tissue (testis): positive staining of nuclei of Leydig cells. (B) Non-tumor liver tissue showing negative staining. (C) Negative staining in HCC. (D) 1+ heterogeneous staining in HCC. (E) 2+ heterogeneous staining in HCC. (F) 3+ diffuse staining in the main tumor (*) and tumor cells in lymphovascular spaces (arrows). Original magnification 200 ×.

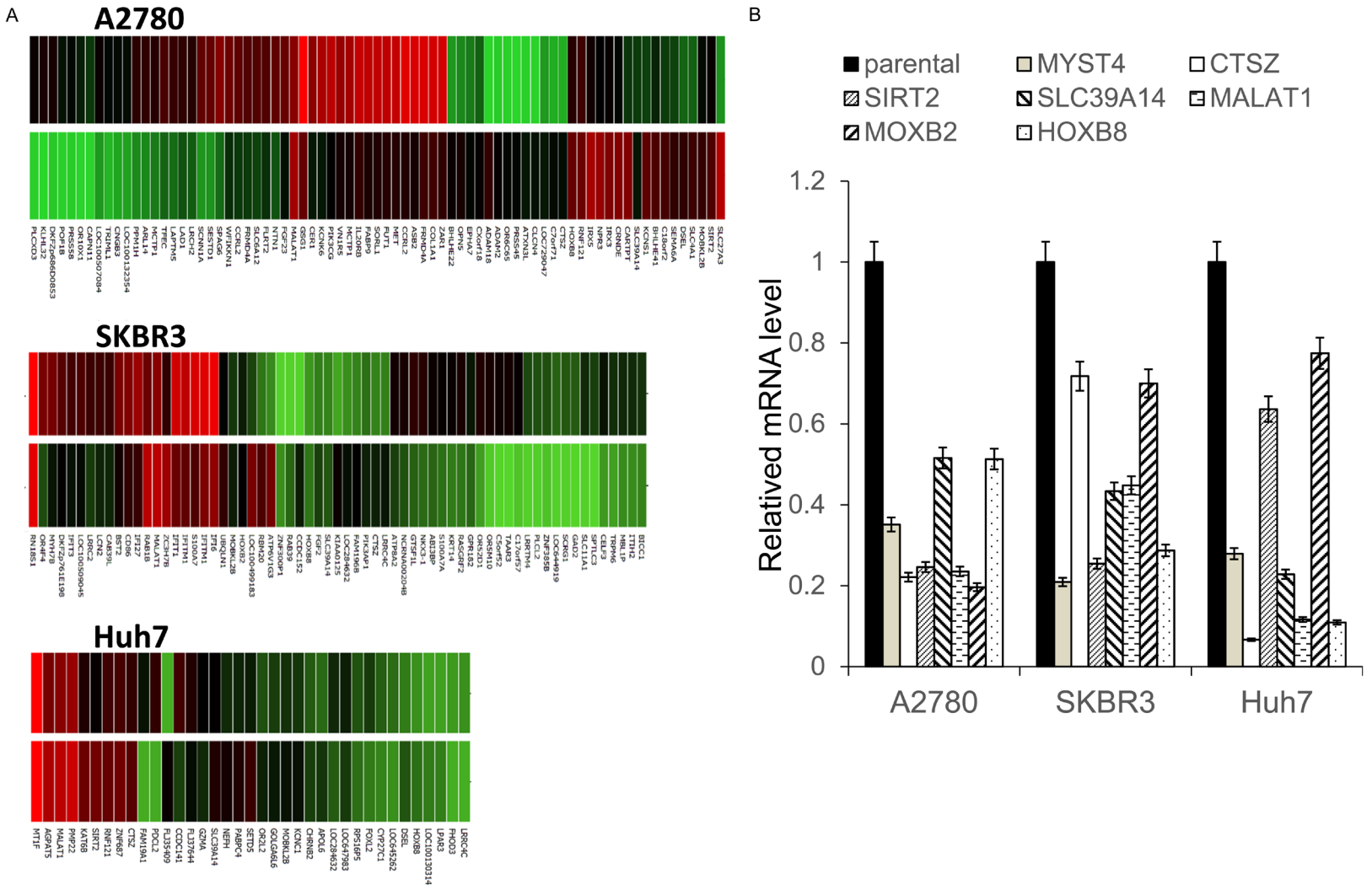

Figure S3. Six critical regulated genes were predicted to be suppressed following MYST4 silencing. MYST4 was silenced using a shMYST4-51 clone in the A2780, SKBR3 and Huh7 cells. A. Through a microarray analysis, 4353 genes passed the 2 × fold change, and 6 critical genes were selected for further investigation. B. The relative mRNA expression levels of all 6 selected genes was measured by an RT-qPCR in the three MYST4 stable knockdown cell lines. Data are presented as the mean ± SD of three independent experiments.